NRC Research Press

ARTICLE

Geotechnical engineering significance of Great Plains polygonal fault system

Andy St-Onge

Abstract: An extensive polygonal fault system (PFS) within fine-grained Upper Cretaceous sediments beneath the Great Plains of North America has implications for geotechnical engineering. Geological well control, outcrop, and three-dimensional seismic data from southeast Saskatchewan exemplify the fault characteristics typically observed within the PFS. The deepest faults are sparse, offset a seismic reflection identified from the Niobrara Formation Govenlock member, and have vertical offsets <2 m. The deformation increases in fault density and vertical offset at shallower depths, reaching 6 faults/km² with up to 30 m of vertical offset. Upper Cretaceous strata throughout the Great Plains area are at or near outcrop, and the extensive PFS faulting and weathering have weakened the rock. This faulting and weakness have been observed and attributed to other factors such as glacial erosion, overconsolidation, swelling bentonite beds, or landslides from toe erosion at topographic slopes. The PFS faulting should be recognized as an extensive process to be considered when undertaking geotechnical analysis on the Great Plains where underlying Upper Cretaceous rocks exist. Engineering implications include road cuts, dam impoundments, building foundations, and natural slumping.

Key words: structural geology, polygonal fault systems, Upper Cretaceous, Saskatchewan, Great Plains.

Résumé : Un système vaste de failles polygonales (PFS) à l'intérieur de sédiments du Crétacé supérieur de grain fin sous les Grandes Plaines d'Amérique du Nord a des implications pour l'ingénierie géotechnique. Des données de contrôle de puits géologiques, des affleurements, et sismiques en trois dimensions du sud-est de la Saskatchewan illustrent les caractéristiques de faille généralement observées au sein du PFS. Les défauts les plus profondes sont rares, et créent un décalage de la réflexion sismique identifié à partir du membre Govenlock de la Formation de Niobrara, et ont des décalages verticaux <2 m. La déformation augmente en densité de faille et en décalage vertical à des profondeurs atteignant 6 failles/km² avec jusqu'à 30 m de décalage vertical. Des couches du Crétacé supérieur dans l'ensemble de la région des Grandes Plaines sont à ou près de l'affleurement et la faille vaste PFS et l'érosion ont affaibli la roche. Cette faille et cette faiblesse ont été observées et attribuées à d'autres facteurs tels que l'érosion glaciaire, la surconsolidation, le gonflement des lits de bentonite ou des glissements de terrain dû à l'érosion aux pentes topographiques. Les failles PFS doivent être reconnues comme un processus important à prendre en considération au moment d'entreprendre une analyse géotechnique sur les Grandes Plaines où existent des roches du Crétacé supérieur sous-jacent. Les conséquences techniques comprennent les routes, barrages de retenue, les fondations des immeubles et de l'affaissement naturel. [Traduit par la Rédaction]

Mots-clés : géologie structurale, systèmes de failles polygonaux, Crétacé supérieur, Saskatchewan, Grandes Plaines.

Introduction

Polygonal faults systems (PFSs) are geological phenomena consisting of coalesced fault traces over a large geographical area. Since their identification by Henriet et al. (1991), interpreting two-dimensional (2-D) seismic data, they have been recognized in over 100 basins worldwide (Cartwright 2011). The faults are formed in fine-grained sediments, without the requirement of external stresses (Lopez et al. 2015). The primary evidential characteristic of PFSs is the polygonal planform geometry of the aggregated fault traces (Fig. 1). As the normal faults increase in vertical offset and lateral extent, the fault traces coalesce. Viewed as a map, the planform fault traces resemble geometrical patterns that can continue for thousands of square kilometres.

Cartwright and Dewhurst (1998) outlined numerous criteria for PFS identification (Fig. 1). There can be layer bound faulting where the strata above and below are undisturbed. The faulting can occur over large areas (up to 0.15 × 10⁶ km² or more). Faults can have up to 100 m of vertical offset with 100–1000 m interfault spacing. Moreover, the faulting can be divided into two or more tiers of strata, with each tier having independent fault offsets and geometries. Sometimes prevalent faults from a lower tier can influence faulting in the upper tier(s). Finally, the fault polarity can switch along the vertical extent of a fault. Also, dips from 45° to 80° characterize the faulting (Cartwright 2011).

The exact causes of PFS fault initiation, fault growth, and the depth of burial at which PFSs initiate are still being investigated (Cartwright 2014). The fractures and faults begin in fine-grained sediments from pure smectitic claystones to almost pure chalks (Cartwright and Dewhurst 1998). However, fault initiation is poorly understood. Goulty and Swarbrick (2005), Cartwright et al. (2003), and Cartwright (2011) provide overviews of processes that have been examined to explain the fault initiation. Downslope gravitational loading has been considered, but it cannot explain PFSs in horizontal basins (Henriet et al. 1991). Syneresis, the chemical expulsion of liquid from a gel and subsequent volumetric contraction, has been proposed (Cartwright and Lonergan 1996). However, Goulty and Swarbrick (2005) argue that syneresis cannot account for all PFS formation, but mudstones with very low coefficients of residual friction can account for the pervasive faulting. Sediment density inversion (Goulty 2008) and overpressure (Roberts et al. 2015) have been considered as possible catalysts for

Received 9 August 2016. Accepted 2 March 2017.

A. St-Onge. PFS Interpretations Ltd., 427 28 Avenue NW, Calgary, AB T2M 2K7, Canada.
Email for correspondence: geophysicist@shaw.ca.

Published at www.nrcresearchpress.com/cgj on xx xxx xxxx.

Fig. 1. Five characteristics (1–5, after Cartwright and Dewhurst 1998) of PFSs identified in Great Plains of North America PFS (St-Onge 2017), and four other representative features (*a*–*d*) that characterize faulting discussed here.

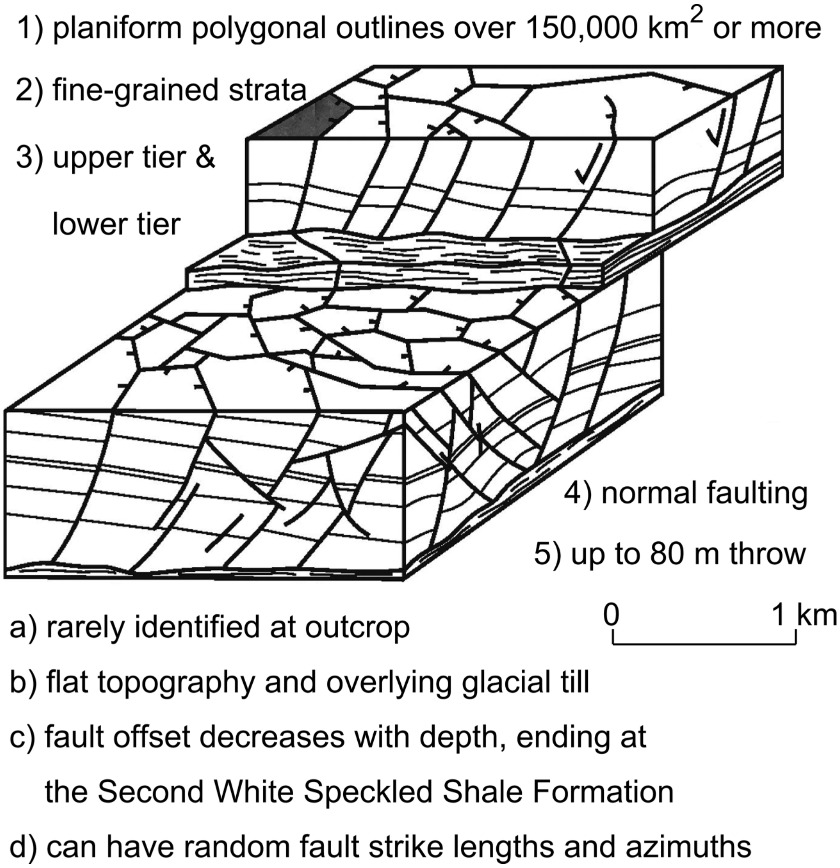

fracture initiation, but there are limitations for either of these to be considered a single initiator for all PFSs. The exact causes of PFS formation are still under investigation (Lopez et al. 2015) and will not be investigated in this analysis, which concentrates on the fault characteristics as observed at shallow depths.

Faulting at or near surface in the Great Plains has been recognized for almost 100 years. Twenhofel (1925) reported on randomly oriented normal faulting in outcrops of the Niobrara Formation in western Kansas (Fig. 2, location 1). He noted that structural variations for the Cretaceous outcrop were due to both structural variation in the beds and lateral variations in Cretaceous bed thicknesses. Townsend (1950) noted "intensely folded and faulted" Tertiary Fort Union Formation strata in northwestern North Dakota and noted that this may indicate deformation of older rocks at depth (Fig. 3). Sauer (1978) provided a review of numerous observations of disturbed preglacial bedrock at various locations throughout Saskatchewan (including Freda Lake; Fig. 3) and recognized that the engineering properties for the disturbed bedrock are weakened. Gendzwill and Stauffer (2006) present seismic data imaging Upper Cretaceous sediment faults at up to ~400 m in depth near Saskatoon (Fig. 2, location 2a) and correlate their formation to a process that resulted in similar faults in open-pit coal mines in southern Saskatchewan (Fig. 2, location 2b; Fig. 3). This is an early report of extensive Upper Cretaceous faulting at depth in Saskatchewan and was attributed to Cenozoic time continental extension.

Davis (1985) described numerous Cretaceous listric normal faults in the Denver Basin (Fig. 2, location 3), almost 10 years before the first presentation of extensive PFS faulting identified using three-dimensional (3-D) seismic data (Cartwright 1994). Since then, researchers at the Colorado School of Mines have identified faults in the Denver Basin that they have attributed to PFSs. Sonnenberg and Underwood (2013) recognized PFSs within the Denver Basin interpreting 3-D seismic data. Kernan (2015) interpreted 3-D seismic data in the Denver Basin and related these faults to Upper Cretaceous Niobrara outcrop in western Kansas (Fig. 2, locations 3 and 4). Maher (2014) presented detailed observations of normal faults in the Niobrara Chalk and Pierre Shale in South Dakota, Nebraska, and Kansas (Fig. 2, locations 5).

The idea of an extensive PFS in central North America has been recently presented (St-Onge 2017). The Great Plains PFS (GPPFS) has been identified in Upper Cretaceous fine-grained sediments throughout the Pierre Shale depositional area (Fig. 2; Table 1). A PFS model would account for extensive faulting over a very large area without the requirement of external stress. The GPPFS area was once covered by the Western Interior Seaway, an inland seaway throughout central North America from Albian to Maastrichtian time (~100–68 million years ago; Witzke and Ludvigson 1994). As discussed in the following text, the Pierre Shale is a thick succession of fine-grained sediments deposited within the inland seaway.

In Saskatchewan, there is a maximum thickness of ~900 m of Upper Cretaceous sediments south of Estevan as the Williston Basin thickens towards the town of Williston, North Dakota. At outcrop, there are numerous examples of Upper Cretaceous fine-grained sediments. For example, the Odanah Member of the Pierre Shale Formation outcrops in the Qu'Appelle Valley south of Esterhazy (Hardenbicker 2014). Truax, Saskatchewan, has a bentonite quarry (bentonite is a soft clay smectite mineral used as an industrial binder for materials). The Saskatchewan government recognizes 14 other Upper Cretaceous siliceous deposits (Saskatchewan Geological Survey 2016) that have been mined or have economic potential in southern Saskatchewan.

Fig. 2. Map of western Canada and northwestern United States showing Williston Basin outline (short–long-dashed line), Upper Cretaceous Pierre Shale depositional area (solid line, modified from Roberts and Kirschbaum 1995), and southern limit of Quaternary glaciations (short-dashed line, after Richmond and Fullerton 1986). References for numbered locations: 1, Twenhofel (1925); 2a, 2b, Gendzwill and Stauffer (2006); 3, Davis (1985); 4, Kernan (2015); 5, Maher (2014); 6, Stantec Consulting Ltd. (2016).

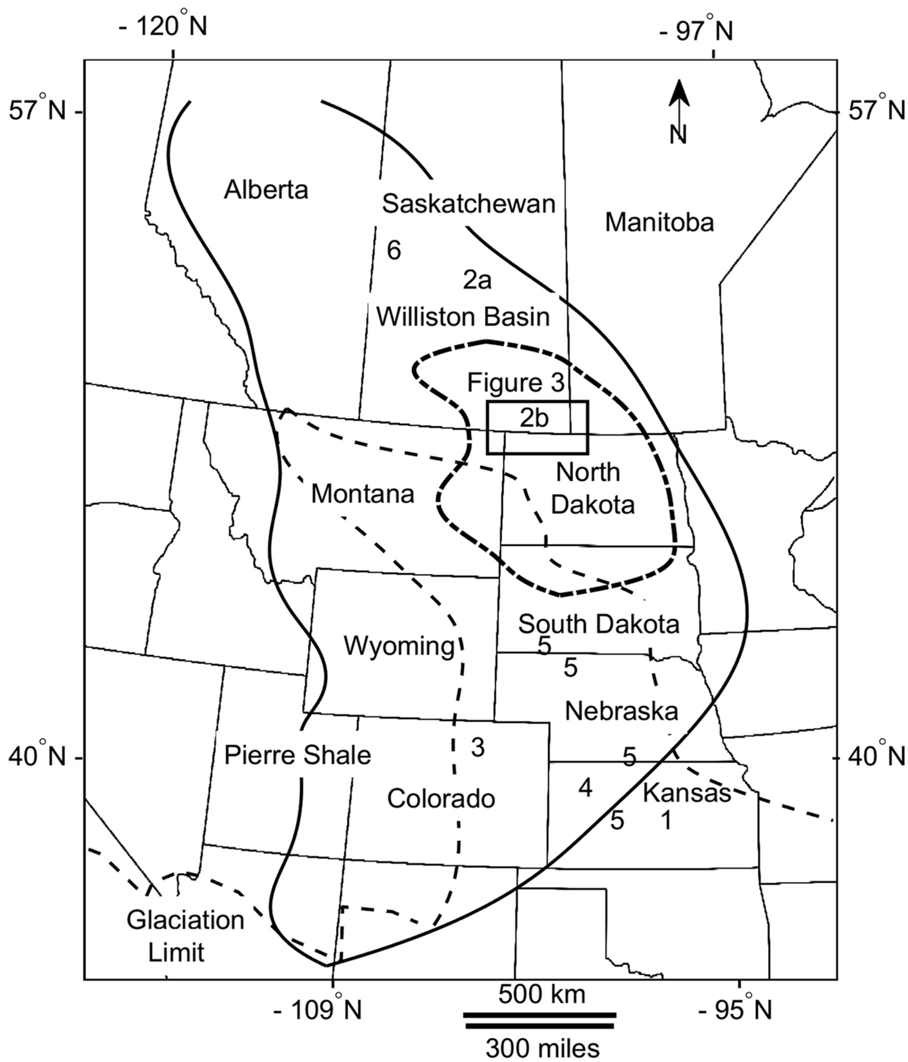

This work presents an interpretation of part of the GPPFS underlying Saskatchewan. Interpretations garnered from analyzing over 70 3-D seismic surveys acquired in an area covering 0.5 × 10^6 km^2 are presented. One 3-D seismic dataset is presented here. Beyond this area, information from wellbore logging and surface geology presented in other reports is interpreted and presented. This work will show that faulting can start at ~700 m in depth and can continue to ground surface. The faulting does not depend upon variations occurring in strata below the Upper Cretaceous such as Middle Devonian salt dissolution or on shallow processes such as glacial action. The goal for presenting this research is to garner acceptance for the polygonal fault system model for Upper Cretaceous sedimentary rocks deposited in the Western Interior Seaway, so the faulting model can be incorporated into geotechnical analyses as appropriate.

Geologic framework

Beneath an expanse of the Great Plains lie sediments deposited in the Upper Cretaceous Western Interior Seaway. The Seaway existed in fairway that extended from the Gulf of Mexico to the Arctic Ocean (Weimer 1960). The Upper Cretaceous Pierre Shale was deposited in the Seaway from late Santonian to early Maastrichtian time (Fig. 2; Table 1) in the Western Interior Seaway over a large area — approximately 2.6 × 10^6 km^2 as defined by outcrop edges. Fine-grained strata were deposited between the Cenomanian and the Campanian time interval during rising and falling sea levels (Schröder-Adams et al. 2001). The western basin edge was bounded by highlands produced by the middle Cretaceous Sevier Orogeny. The eastern basin edge was bounded by Appalachia (Bertog 2010).

The Pierre Shale was first described by Meek and Hayden (1862) along the Missouri River near the town of Pierre, North Dakota (Hanczaryk and Gallagher 2007). The shale was of interest partly because of the large amount of fossils in the outcrops in North Dakota and Montana (Leonard 1911). The shale can reach a maximum thickness of over 365 m (Hargrave 2007) southeast of the Black Hills in South Dakota. Schultz et al. (1980) analyzed and described the composition and properties of 1350 Pierre Shale samples from Montana, North Dakota, and South Dakota. Clay minerals represented 53% of the total bulk volume of the samples, and clay minerals were present in all of the samples. The Pierre Shale encompasses three formations and their subunits in Saskatchewan (Table 1). These subunits were used when correlating

Fig. 3. Southeast Saskatchewan and North Dakota index map for areas presented in this study.

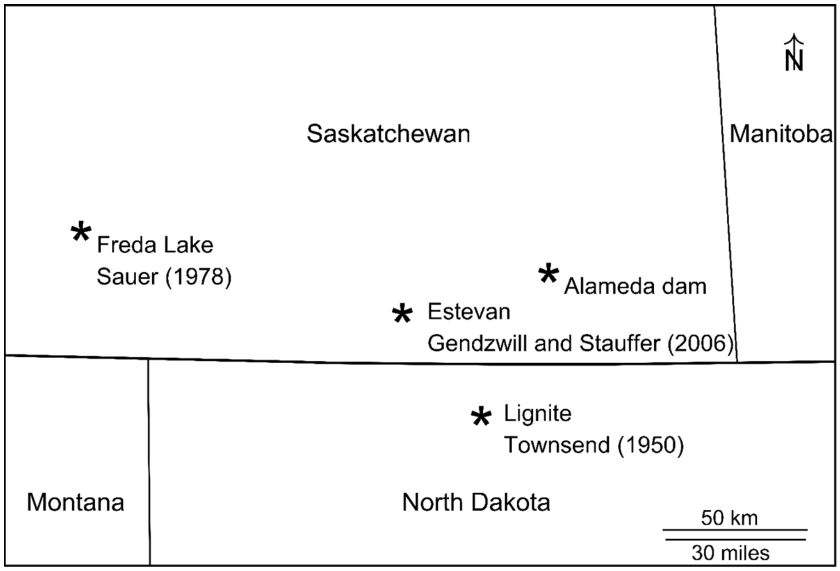

sonic logs to seismic data in this study as an aid to try to date the faulting discussed in the PFS.

Outcrop of the Pierre Shale can be sporadic in the Great Plains area, which has relatively flat topography. Erosional incisions along river valleys can expose Pierre Shale, but these outcrops can be confounded by complex slumping (Erskine 1973). In the north part of the Great Plains, there have been numerous periods of glaciations during the Pleistocene Epoch (2.6 million to 10 000 years ago; Hallberg and Kemmis 1986; Fig. 2). Glaciers have extended as far south as Colorado, and glacial till can mask the Upper Cretaceous (and sometimes Tertiary sediments; Roberts and Kirschbaum 1995). This can require wellbore drilling and (or) excavation to expose the underlying Cretaceous beds. Conventional boreholes for oil and gas well drilling in the area typically do not sample or log the first ~200 m of borehole (due to the presence of surface casing, cost associated with logging, and the lack of regulatory requirement to do so). The Water Security Agency of Saskatchewan has a website (available from www.wsask.ca) that provides downloadable maps, reports, cross sections, and wellbore data for hundreds of shallow wells throughout the province that have logged shallow stratigraphy. For specific areas, glacial till and Tertiary sediment thicknesses can be obtained by investigating their website.

As discussed earlier, geologists and engineers have recognized near-surface deformation of Upper Cretaceous and shallower beds at outcrop within the Great Plains. A lot of this deformation has been interpreted to be caused by glacial action. Sauer (1978) and Kupsch (1962) proposed an "ice-thrust" ridge model where glaciers folded and sheared drift and frozen bedrock in western Canada. Some of the Upper Cretaceous deformation has been interpreted as ice-thrust ridges. This interpretation can involve thicknesses of 100 m or more of glacial till and bedrock sediments in Saskatchewan. A key feature of the model is a lower limit of permafrost (interpreted to be ~165 m thick from surface), over which the frozen competent strata can be overthrust onto older beds, especially when glaciers encounter up-slope topographic elevations. Sauer (1978) presented a geological cross section that includes the Freda Lake area of Saskatchewan showing thrust ridges mapped at surface and attributed the change in drift thickness to ice thrusting (Fig. 3). Byers (1959) analyzed surface deformation in the Upper Cretaceous and shallower beds near Claybank, Saskatchewan. He interpreted over 60 m of vertical bed deformation in the Upper Cretaceous strata and attributed this to glacial processes. Townsend (1950) described similar deformation in overlying Paleocene Fort Union Formation outcrop near Lignite, North Dakota. However, this deformation was attributed to deeper geological processes unrelated to glacial workings.

Pierre Shale geotechnical framework

Since the Pierre Shale is at or near outcrop throughout the Great Plains area, the geotechnical properties of the rock have been analyzed by others to determine its in situ properties. A number of the limitations of these analyses have been presented by Peterson (1958), who notes that the results of laboratory strength tests do not correlate well with field behavior. The most reliable indicator of the properties of the shale is the water content. The shales are overconsolidated from the previous weight of glaciers or eroded overburden; this can lead to movement after excavation (Peterson 1958). The shales have bentonite layers that swell when exposed to water (Ito and Azam 2009). The angle of residual friction in bentonite layers with high smectite content can be significantly reduced (Nichols 1992). Weakened shear zones interpreted to be from ice thrusting have been observed in Upper Cretaceous rocks (Cruden and Tsui 1991). Pre-existing fault and joint planes have been related to excessive rebound deformations, landslides, and roof falls in tunnels (Nichols et al. 1986).

Despite numerous analyses to determine the geotechnical characteristics of the Pierre Shale, engineering uncertainty still exists. Engineers have been surprised by unforeseen movements in the Upper Cretaceous clays in the Great Plains area since the early 1800s (Brooker and Peck 1993). In 1882, an excavation was made in Paleocene rock for a railway bridge across the Missouri River at Bismarck, North Dakota. A major landslide developed after the excavation. During excavation for the construction of the Oahe Dam in the 1950s on the Missouri River 16 km northwest of Pierre, South Dakota, 0.3 m of vertical ground movement was observed (Nichols 1992). Furthermore, rebound displacements were noted 1 month after excavation (Underwood et al. 1964). These were described as rebound displacements along pre-existing steeply dipping fault planes that were detected over 3 days (Nichols 1992). Myers et al. (1980) investigated remote sensing applications to monitor the Pierre Shale in South Dakota. Landslides, water movement along fault traces, and slope stability problems at cut and fill sections were all detrimental processes attributed to the Pierre Shale. Finally, a recent oil pipeline rupture in the Saskatchewan River Valley (Fig. 2, location 6) was attributed to a complex rotational rock slide in "weak" Cretaceous Lea Park Formation

Table 1. Stratigraphic nomenclature used for this work.

Epoch	Formation	Age (Ma)	Picks	Elevation at Alameda Dam (m)	PFS fault characteristics at Alameda Dam: Throw (m)	Strike	Dip angle (°)	Length (m)	Fault density (faults/km^2)	Comments
Quaternary	Glacial Drift	Pleistocene	2.6	500	Max 80					Shear zone noted at base of drift (Mittal and Rahman 2000)
Tertiary	Ravenscrag	Paleocene	65	450	Unknown					Elevation estimated from tests holes available at www.wsask.ca
Late Cretaceous	Eastend			400						
Late Cretaceous	Montana Group (homotaxial to the Pierre Shale); Bearpaw Formation	Maastrichtian	72.1							
Late Cretaceous	Montana Group; Bearpaw Formation; Demaine member									Not deposited?
Late Cretaceous	Montana Group; Bearpaw Formation; Sherrard member	Campanian	74.7	300						
Late Cretaceous	Montana Group; Bearpaw Formation; Matador member									
Late Cretaceous	Montana Group; Bearpaw Formation; Broderick member			230	5.0 +12/−2	Directional	30–80	340 ± 250	~4	Average offset of 5.0 m; most dips are 40° –50°
Late Cretaceous	Montana Group; Bearpaw Formation; Outlook member									
Late Cretaceous	Montana Group; Belly River									
Late Cretaceous	Montana Group; Lea Park		79?	125	3.4 ± 1.5	Random	30–80	Arcuate	~6	Average offset of 3.4 m; most dips are 40°–50°
Late Cretaceous	Montana Group; Alderson (Milk River)		83.6	90						
Late Cretaceous	Colorado Group; Niobrara; Niobrara	Santonian	86.3	−20						
Late Cretaceous	Colorado Group; Niobrara; Govenlock	Coniacian	89.8	−95	Up to 2		50	Up to 500	<<1	
Late Cretaceous	Colorado Group; Carlisle			−177						
Late Cretaceous	Colorado Group; Morden	Turonian								
Late Cretaceous	Colorado Group; 2WS		93.9							
Late Cretaceous	Colorado Group; Belle Fourche									
Late Cretaceous	Colorado Group; Fish Scales	Cenomanian	100							

Note: The correlations are referenced to Christopher and Yurkowski (2004) and Cobban et al. (2006).

Fig. 4. Perspective Google Earth view of Alameda Dam looking north. Dam construction completed in 1994. 3-D seismic dataset presented in this paper imaged an area ~14.5 km² about 6 km northeast of the dam at a confidential location. Wells at Dominion Land Survey locations 3-1-4-3W2 and 2-1-4-3W2 drilled to deeper formations in 1980 (see https://en.wikipedia.org/wiki/Dominion_Land_Survey). Map data: Google, DigitalGlobe.

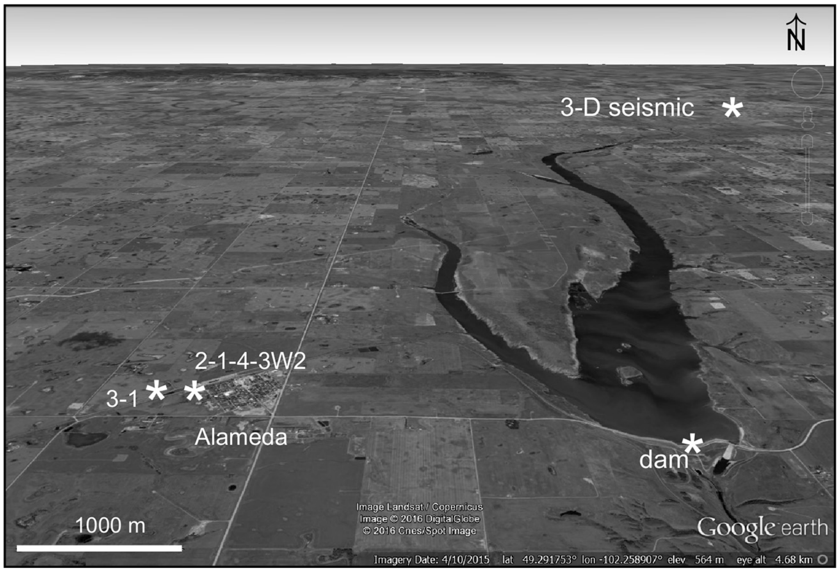

shales with fractures and shear zones (Stantec Consulting Ltd. 2016).

Alameda Dam

The Alameda Dam was constructed in 1991–1995 as part of the Rafferty–Alameda project to control downstream flooding from the Moose Mountain Creek near Oxbow, Saskatchewan (Figs. 3, 4). The dam is a 42 m high and 1250 m long earth dam with a full supply level at 562 m elevation of 105 500 dam³ (Quinn et al. 2014). Construction was halted during construction of the dam because of unexpected movements in the high plasticity clay shale bedrock ~30 m below a glacial till construction base. The movements were partially attributed to movement of pre-sheared slip planes in the clay shale strata. Slope inclinometers indicated deformations in a shear zone at ~498 m elevation (Mittal and Rahman 2000). This is interpreted to be the glacial till – clay bedrock contact (Quinn et al. 2014). Stabilizing berms were added before dam completion.

Seismic data and interpreted datasets

There are a number of 2-D and 3-D seismic datasets acquired within the Great Plains area for deeper oil pool targets that have imaged the shallower GPPFS. In southeast Saskatchewan, most seismic data acquisition geometries are designed to image Mississippian-aged reservoirs at 1000 m in depth or more. The shallowest targeted zone to image is the Cretaceous Second White Speckled Shale (2WS), a consistent marker bed that provides a regional seismic reflection. It is also the zone of the deepest depth of faulting observed in this study at up to 700 m in depth. As a result, southeast Saskatchewan seismic data quality can be poor in the Upper Cretaceous beds (see Appendix A). Also, the acoustic impedance contrast between these beds can be small, resulting in weak or no seismic reflections to interpret.

Most of the 3-D seismic datasets interpreted for this study were recorded using geophones spaced 50 m apart in lines 200–300 m apart. The dynamite sources, each 0.5–1.0 kg, were loaded into 12–18 m deep tamped holes drilled 50 m apart; the source lines were 300–350 m apart. The seismic data were interpreted by matching the seismic data to sonic log profiles from wellbores. This determined the correlations of the geological horizons with the recorded seismic reflections. Key reflections were interpreted and mapped to identify geological bed structure and faulting geometries.

Observations and data interpretation

A two-well cross section (Fig. 5) shows missing Upper Cretaceous section in a wellbore drilled ~3 km west of the Alameda Dam. The two wells are only 290 m apart and display a 31 m isopach difference in the Bearpaw Formation above the lower Outlook member of the Bearpaw Formation, yet otherwise have correlative resistivity log signatures. The gamma ray logs (not shown) for both of these wellbores indicate fine-grained lithologies throughout the Upper Cretaceous. The loss of section is interpreted to occur after the deposition of the base Tertiary Ravenscrag Formation, as that contact is vertically offset by the same amount. Little change in log signature is observed below the lower Outlook member. This is interpreted that the loss of the Upper Cretaceous sediments is not caused by deeper processes such as Middle Devonian Prairie Evaporite salt dissolution. The base of the uppermost Cretaceous Eastend Formation contact at ~400 m elevation is corroborated by a cross section of water well and test well logs available from the Water Security Agency website (www.wsask.ca). The cross section and mapping estimates the top of the Eastend Formation at ~430 m, and the top of the Ravenscrag Formation at ~500 m. This is the elevation where slope inclinometers at the dam indicated a shear zone.

The 3-D seismic data presented here are within 5 km of the north end of the Alameda Dam (Fig. 4). The dataset was used to construct a two-way traveltime map for the reflection from the impedance contrast associated with the Outlook member of the Bearpaw Formation (hereafter referred to as the "lower Outlook seismic reflection"; Figs. 5–8). This reflection images a bed contact ~400 m below ground surface. It is the shallowest continuous reflection that is imaged on the seismic data. Lower Outlook seismic reflection faults with as much as 17 m of vertical offset are evident on the map and the seismic line (Figs. 6–8). There are no shallower continuous seismic data reflections observed. The average fault density for the lower Outlook seismic reflection is ~4 faults/km². The lower Outlook seismic reflection images faults that have a mean strike length of ~338 m and a mean offset of

Fig. 5. Two-well cross section ~3 km (2 mi.) west of Alameda Dam (Fig. 4). Wells are only 290 m apart. There are ~31 m of Upper Cretaceous sediments missing in well 2-1-4-3W2 above lower Outlook member (l. Outlook mbr.) of Bearpaw Formation (see Table 1). This member and Lea Park Formation, Govenlock member of Niobrara Formation, and Second White Speckled Shale Formation (2WS) all correspond to interpreted seismic reflections (Figs. 6–10). This interpretation corroborates a top Ravenscrag to Eastend isopach of ~120 m (Water Security Agency; available from www.wsask.ca).

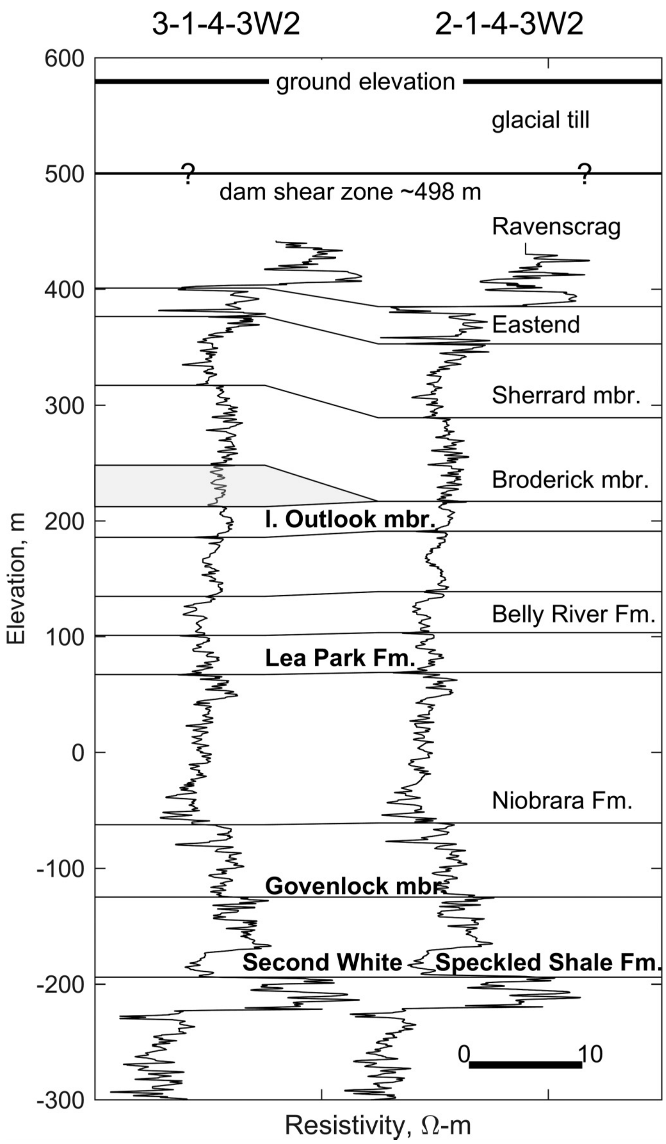

5.0 m (Fig. 7). The faulting is aligned in two directions, NNW and NE, and most of the fault dips are between 40° and 50°.

The seismic line (Fig. 8) shows a number of small vertical offsets faults in the seismic reflection associated with the deeper Lea Park Formation, hereinafter referred to as the "Lea Park seismic reflection". The faults traces are evident on the Lea Park two-way traveltime map (Fig. 9). The average fault density for the Lea Park zone is ~6 faults/km^2, with an average measured strike length of 315 m and a mean offset of 3.7 m (Fig. 10). In the Alameda area, the Lea Park is at ~100 m elevation (460 m in depth). With increased depth below the Lea Park, the faulting lessens in frequency and vertical offset until only minor faulting (<2 m offset) is observed at the Coniacian Govenlock reflection (Table 1).

As discussed earlier, outcrop of Tertiary and Cretaceous beds can be sporadic. However, Townsend (1950) noted deformation of the Paleocene Fort Union Formation at outcrop near Lignite, North Dakota (Figs. 3, 11). He attributed this deformation to deeper (and unspecified) geological processes. There are over 50 wellbores within a mile of the outcrop that penetrated Cretaceous beds. A comparison of the two wellbores shown in Fig. 12 indicates 10 m of positive relief at 509 m elevation, decreasing to <4 m of positive relief at 83 m elevation due to an extra 6 m of extra undifferentiated Pierre Shale Formation strata in the NENE12 wellbore. Vertical movement caused by the PFS could have caused these structural differences. No glacial processes have been observed at these depths.

A four-well cross section was constructed near Freda Lake, Saskatchewan (Figs. 13, 14). The gamma ray logs (not shown) for these wellbores indicate fine-grained lithologies throughout the Upper Cretaceous. The surface geology for this area was examined by Sauer (1978) who noted numerous folds and thrusts at outcrop. In the subsurface, the four logs are correlative in depth and log character below ~250 m elevation. The highest continuous correlation at 455 m in 1-32-4-18W2 has over 20 m of structural variation on the cross section. These variations are almost 300 m below ground surface. The 7-32-4-18W2 wellbore has ~55 m of shaded section in Fig. 14 that indicates missing section in either 9-31-4-18W2 or 5-32-4-18W2. Note the consistent strata in the four wellbores below ~200 m elevation. Although no 3-D seismic datasets were available for interpretation at these well locations, it is interpreted that the bed variations could have been caused by the GPPFS.

Discussion

The following discussion presents a number of statements that summarize the data observations made here. Following these statements are brief discussions about the geotechnical engineering implications for each statement.

Statement: There is faulting prevalent within fine-grained Upper Cretaceous sediments deposited within the Great Plains area

All of the wellbores interpreted here and used to interpret the seismic data presented here indicate fine-grained lithologies. This is based upon gamma ray or spontaneous potential logs or core and sample summaries for the wellbores examined in this study. This is consistent with the fine-grained Upper Cretaceous lithologies summarized by Schultz et al. (1980). Townsend (1950) noted the "intensely folded and faulted" Tertiary Fort Union Formation in NW North Dakota was underlain by 1000 ft (305 m) of undifferentiated Pierre Formation shale. Sauer (1978) noted, in his study of glacier ice thrusting, all deformed bedrock in Saskatchewan is clay shale or weakly cemented bedrock. It is interpreted here that the clay shale is fine grained. Gendzwill and Stauffer (2006), in their analysis of Upper Cretaceous faulting throughout Saskatchewan, characterized faulting as occurring in fine-grained marine shales and very fine grained to medium-grained muddy sandstones. Sonnenberg and Underwood (2013) reported PFS faulting in the Denver Basin specifically in fine-grained Upper Cretaceous strata. Finally, Maher (2014) presented observations of normal faults in the Niobrara Chalk and Pierre Shale in South Dakota, Nebraska, and Kansas that he described as having fine-grained mud rock lithologies.

Implication

Because of the prevalence of faulting and fracturing within fine-grained Upper Cretaceous sediments deposited within the Great Plains area, the entire area should be considered a potential host for a polygonal fault system. If faulting is a geotechnical concern, detailed surface geology and geophysical methods such as seismic data targeting the near surface should be considered.

Fig. 6. Lower Outlook seismic reflection elevation map corresponding to lower Outlook member of Lea Park Formation (Fig. 5). Faults indicated by computed gradient values (Appendix B). Largest gradient values correspond to ~17 m of vertical throw. Average acoustic wave velocity is 2000 m/s; 1 ms ~1 m. [Colour online.]

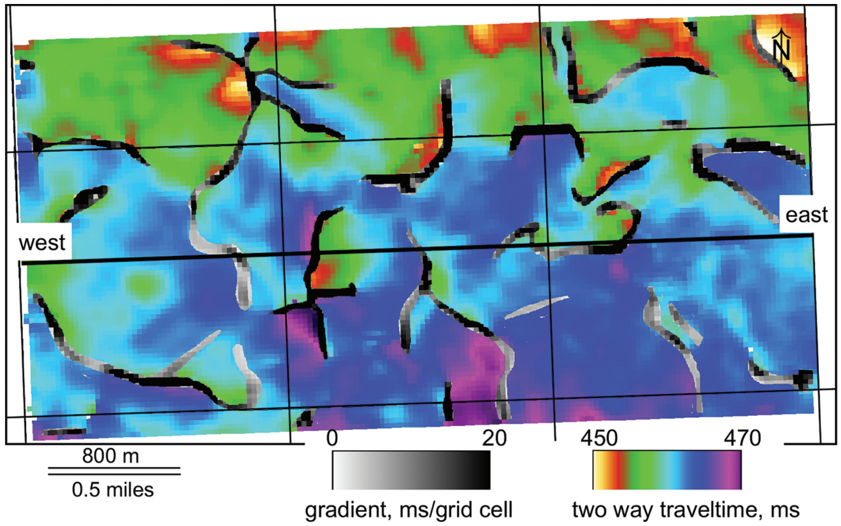

Fig. 7. Fault strike length, azimuth, and maximum vertical offset for 50 lower Outlook seismic reflection faults (30 of 50 larger offset faults identified in Fig. 6). Fault density is ~4 faults/km²; faults have predominant strikes to NNW and NE directions. Black lines at strike angles 49° and 139° observed by Stauffer and Gendzwill (1987) as predominant strike angles for Upper Cretaceous fractures and stream patterns measured throughout Saskatchewan, NE Montana, and NW North Dakota. *n*, number of faults.

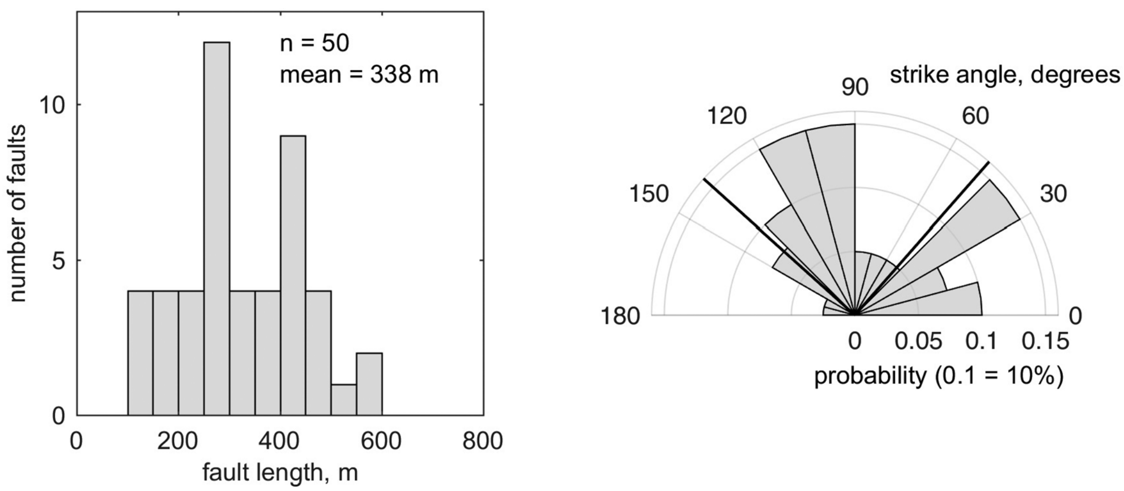

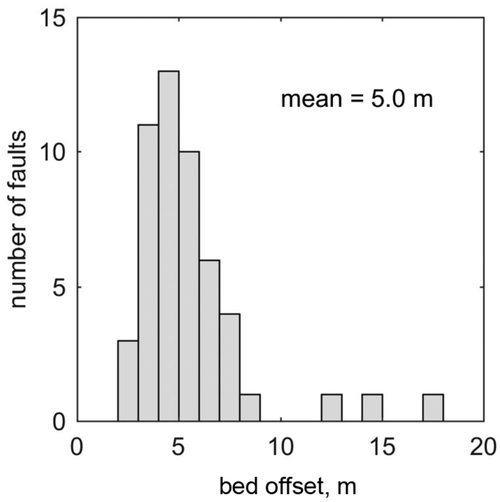

Fig. 8. West to east vertical slice through seismic survey showing some of the otherwise subhorizontal reflections offset by interpreted PFS normal faults. Faulting increases above lower Outlook reflection, which is shallowest continuous reflection within survey. Faulting is evident down to Lea Park Formation reflection, over 500 m below ground surface.

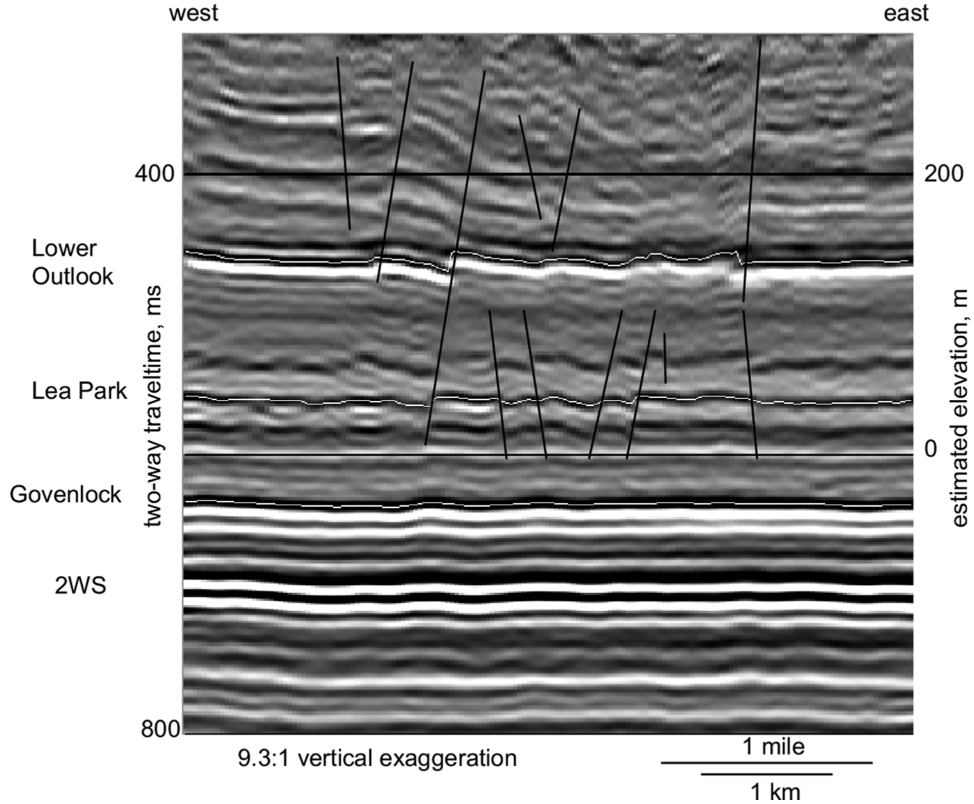

Fig. 9. Lea Park seismic reflection two-way traveltime map. Fault density for Lea Park seismic reflection is ~6 faults/km², more than lower Outlook seismic reflection, but faults have lower average vertical offset of 3.4 m (versus 5.0 m for lower Outlook reflection). [Colour online.]

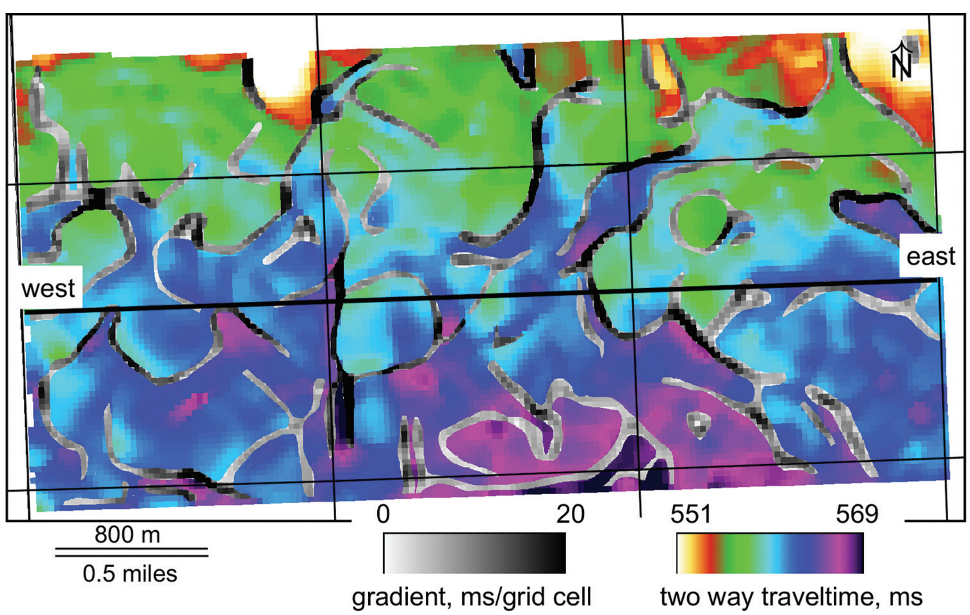

Statement: The faulting is consistent with PFS faulting characteristics

The faulting presented here and by others is consistent with the characteristics identified by Cartwright and Dewhurst (1998). The faulting is layer bound, limited to seismic data reflections above the Govenlock member of the Niobrara Formation in this work (Figs. 1, 8). The faulting occurs over an area >1.0 × 10^6 km² (Fig. 2). The largest vertical bed offset presented here is ~31 m (Fig. 5). This is consistent with faults observed in coal beds at outcrop in Paleocene Fort Union Formation coal beds with offsets of 21 m (Gendzwill and Stauffer 2006). The faulting observed on the lower Outlook and Lea Park seismic reflection maps have offsets up to 17 m, with fault strike lengths averaging less than 800 m. All of these characteristics are consistent with PFS identification.

Fig. 10. Fault strike length, azimuth, and maximum vertical offset for Lea Park seismic reflection faults (Fig. 9; arcuate faults are broken down into 30° strike increments). Faults have no predominant strike direction.

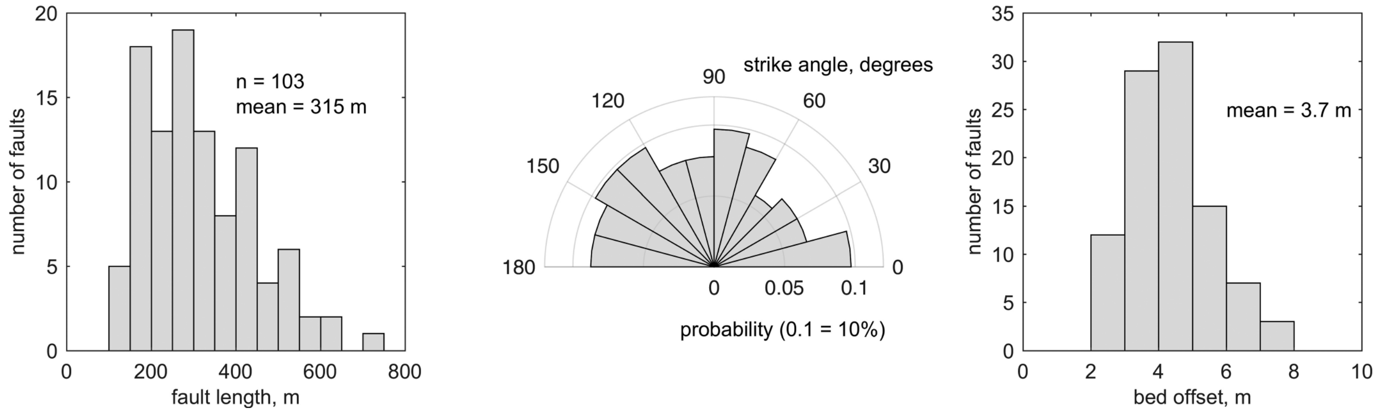

Fig. 11. Google Earth image showing Tertiary bed outcrop at Lignite, North Dakota, studied by Townsend (1950) who mapped 3 m displacements in high-angle faults of Paleocene Fort Union Formation beds. Folds with ~13 m of vertical relief and coal beds dipping 30° were also noted. NENE 12-161N-92W wellbore is ~860 m NE of SESW 6-161N-91W wellbore. Map data: Google, DigitalGlobe.

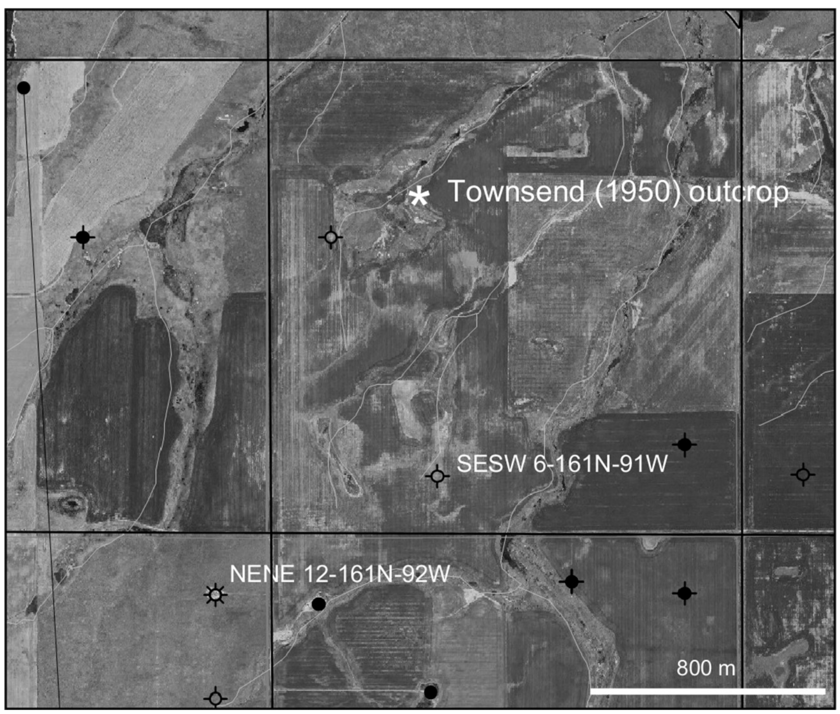

Note the near-random orientation of the Lea Park seismic reflection faults (Fig. 10) as compared with the NNW- and NE-striking orientation for the shallower lower Outlook seismic reflection faults (Fig. 7). Sonnenberg and Underwood (2013) observed near-random fault distribution in the Niobrara Formation in the Denver Basin, consistent with the observations presented here. Stauffer and Gendzwill (1987) observed streams and fractures in Upper Cretaceous sediments at outcrop that strike at predominant angles almost identical to the major alignment noted for the lower Outlook seismic reflection (Fig. 7). Extensional tectonics caused by the westward motion of the North American continent, as postulated by Stauffer and Gendzwill (1987), may be the cause of the lower Outlook seismic reflection orientations. This similarity is under further investigation with additional seismic datasets.

Implication

If the faulting is caused by a PFS, the main implication is that PFS faulting may scale with magnitude (Sonnenberg and Underwood 2013). Faults observed in the range of hundreds of metres on seismic data may imply fractures at a metre and centimetre scale. This could impact the in situ material strength.

Statement: The faulting is complicated and can be masked by near-surface cover

The extensive faulting observed interpreting the seismic and wellbore data are partially masked by glacial till and other surface deposits such as Quaternary cover (i.e., recent sediments deposited along waterways). The faults present at Alameda in the two wellbores (Fig. 5) are not observed at the surface. The complicated geometries observed on the seismic data two-way traveltime maps (Figs. 6, 9), including fault densities, are not observed at the surface.

Implication

Extensive subsurface faulting may be masked by glacial till and other surface deposits.

Fig. 12. Two-well cross section from Lignite area (Fig. 11). There are ~10 m of vertical offset in uppermost Upper Cretaceous Pierre Shale Formation beds, compared with ~3.4 m of vertical offset ~400 m below shallower interval. Lower Campanian Eagle Sandstone Formation zone has been identified in NENE12 at –283.7 m (correlated to –324 m in NESWSW2-161N-93W, about 13 km west), below log depths presented here. δ, thickness change.

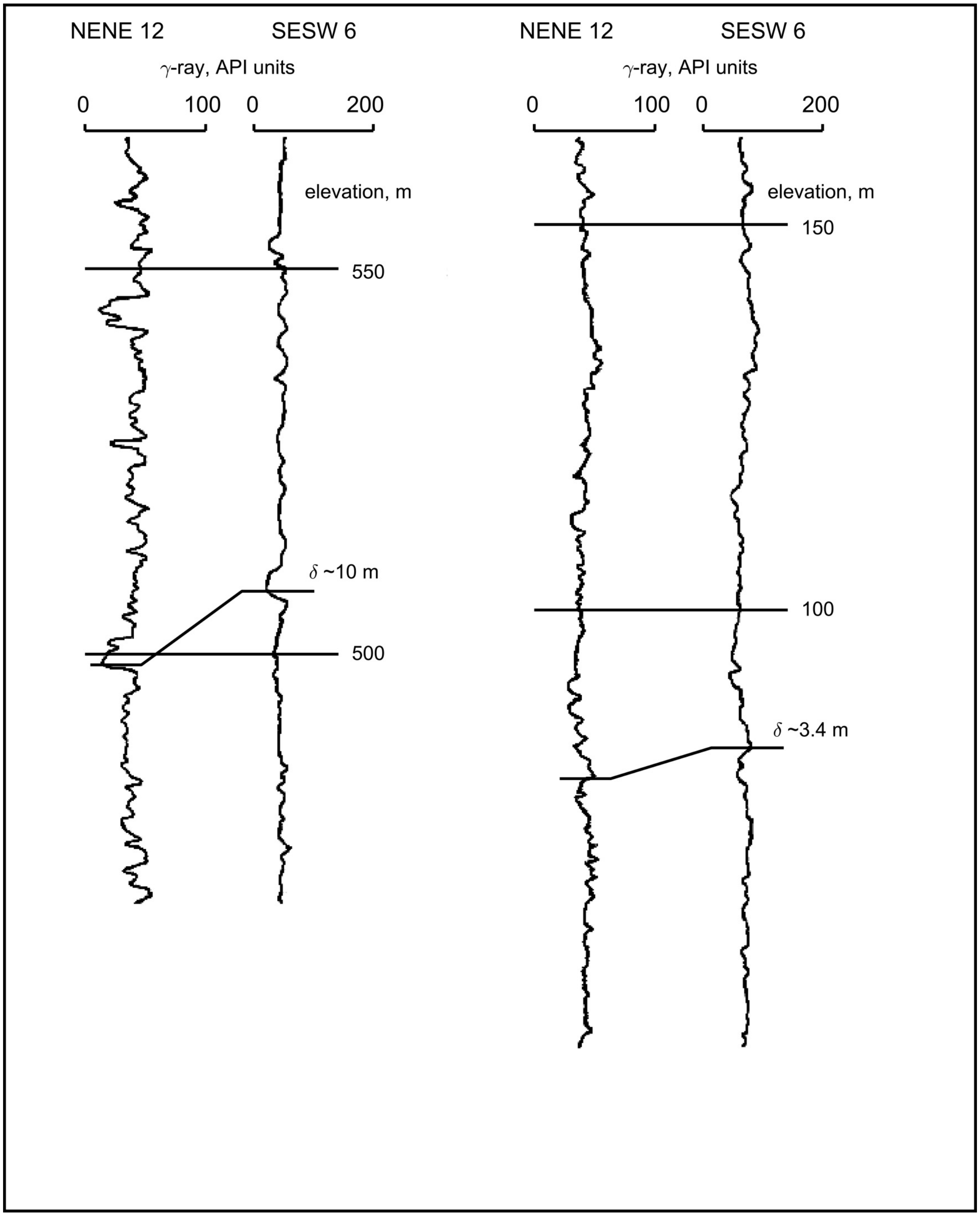

Statement: Faulting attributed to other processes may be PFS faulting

Deeper processes such as the dissolution of Middle Devonian Prairie Evaporite (over 100 m in thickness, ~1540 m below the Turonian 2WS at Estevan, Saskatchewan), as discussed by Christiansen (1967) in the vicinity of Saskatoon, could not have caused the faulting presented. The Prairie Evaporite is not disturbed at the locations of the data shown here. Also, the reflections from Lower Cretaceous and Jurassic beds show undisturbed sediments.

Slumping (normal faulting, usually into a one-sided depression such as a river valley) has many similarities to a PFS. Polygonal fault system formation begins with slumping, but in 3-D. Both slumping and PFS cause fractures, faulting, and associated changes to shear properties. Sauer et al. (1990) examined unweathered Cretaceous clay in Saskatchewan and attributed glacial shear as the cause of clay softening to a maximum depth of 140 m. Cartwright (2011) argues that diagenetically induced shear failure of fine-grained sediments is the in situ cause of the

Fig. 13. Freda Lake (see Fig. 3) well base map showing four-well cross section (Fig. 14). Top ~500 m of 3-32-4-18W2 wellbore was presented in a cross section by Sauer (1978), who attributed glacial drift isopach variations in this wellbore to glacial ice thrusting.

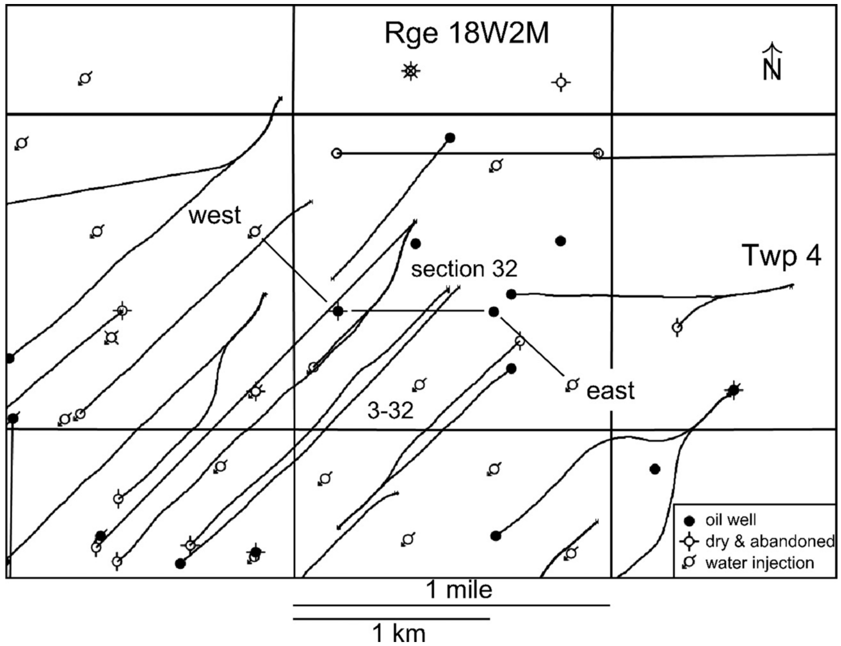

formation of shear fractures and normal faults that initiate and form PFSs.

Implication

Faulting attributed to other processes such as late Middle Devonian salt dissolution and slumping may be due to PFS faulting.

Statement: The PFS model discussed here can be used in other areas

A PFS model at or near outcrop is rare; the one other example of an extensive PFS at outcrop is in the western desert of Egypt (Tewksbury et al. 2014). Most of the PFSs have been identified on offshore margins (Cartwright 2011), where wellbore spacing is sparse (on the order of magnitude 1000 times less than the Great Plains area).

Implication

A PFS model within the Great Plains has been sampled by at least 300 000 wellbores. Work done to further this model can lead to a better understanding of PFS processes.

Statement: Geotechnical properties are best measured in situ

Some geotechnical properties of the Pierre Shale depend upon the amount of fracturing and faulting in the rock. Joints and faults in the Pierre Shale may be unfilled, healed (cemented), or filled, and the overall shear strength can be greatly affected by the state of the joint surfaces (Goodman 1976). There is some evidence that the fractures are open in the subsurface. The hydraulic conductivity of the Pierre Shale is thought to be affected by the presence of subsurface fractures (Shaw and Hendry 1998).

Implication

If the geotechnical properties are best measured in situ, it may take some work such as finite element modelling to characterize the PFS faulting and fracturing in a predictive model for rock mechanical behavior.

Statement: The faulting has implications for present-day engineering projects

During construction of the Alameda Dam in the 1990s, displacements of the clay shale bedrock were noted when the reservoir was initially constructed. Further displacements occurred in 2011, when the dam was surcharged above its full supply level during spring runoff (Quinn et al. 2014). Engineering work showed that the dam stability was influenced by "3-D effects" of clay shale displacement, especially when the dam was surcharged. As a result, it was recommended that the reservoir level be lowered to full supply level. Further analysis and modelling showed that the overall stability of the dam was satisfactory.

Cruden et al. (1995) reported on the reactivation of Upper Cretaceous slides into a 100 m deep valley after 3 years of heavier than normal precipitation at Edgerton, Alberta. Geotechnical analysis for foundation investigations (Underwood et al. 1964) and geotechnical investigations conducted in the Pierre Shale by the United States Geological Survey (Nichols et al. 1986; Collins et al. 1988) indicate that continuing differential rebound displacements are influenced by pre-existing fault planes. Engineering practice used to mitigate time-dependent rebound damage to highways recently constructed over pre-existing faults in the Pierre Shale of South Dakota has not been completely successful (Collins et al. 1988).

Ground movement continues today on the Great Plains. Some residents in the Qu'Appelle Valley northwest of Regina, Saskatchewan, have experienced cracked and shifting basement foundations in homes built on the edge of a river valley with Upper Cretaceous sediments near outcrop (CBC News 2011). A similar problem arose in the spring of 2016 ~23 km northwest of Deer Valley at Regina Beach (CBC News 2016).

Implication

Large-scale geotechnical engineering projects will continue to occur in the Great Plains area, and subsurface investigation for faulting may be required to help predict ground movement.

Conclusions

This paper has shown that the interpretation of 3-D seismic data, wellbore logs, and surface geology corroborate previous work to exemplify the faulting characteristics of an extensive PFS within the Great Plains area. The PFS characteristics are consistent with others identified throughout the world. The normal faults in the PFS could have been reactivated and expressed as rebound faults and slumping fault traces. Polygonal fault system

Fig. 14. Four-well cross section from Freda Lake, Saskatchewan area (Fig. 13). Bedding is almost continuous at elevations below 200 m. Above 200 m, there are structural variations of as much as 30 m in Cretaceous beds and interpreted Tertiary bed contact.

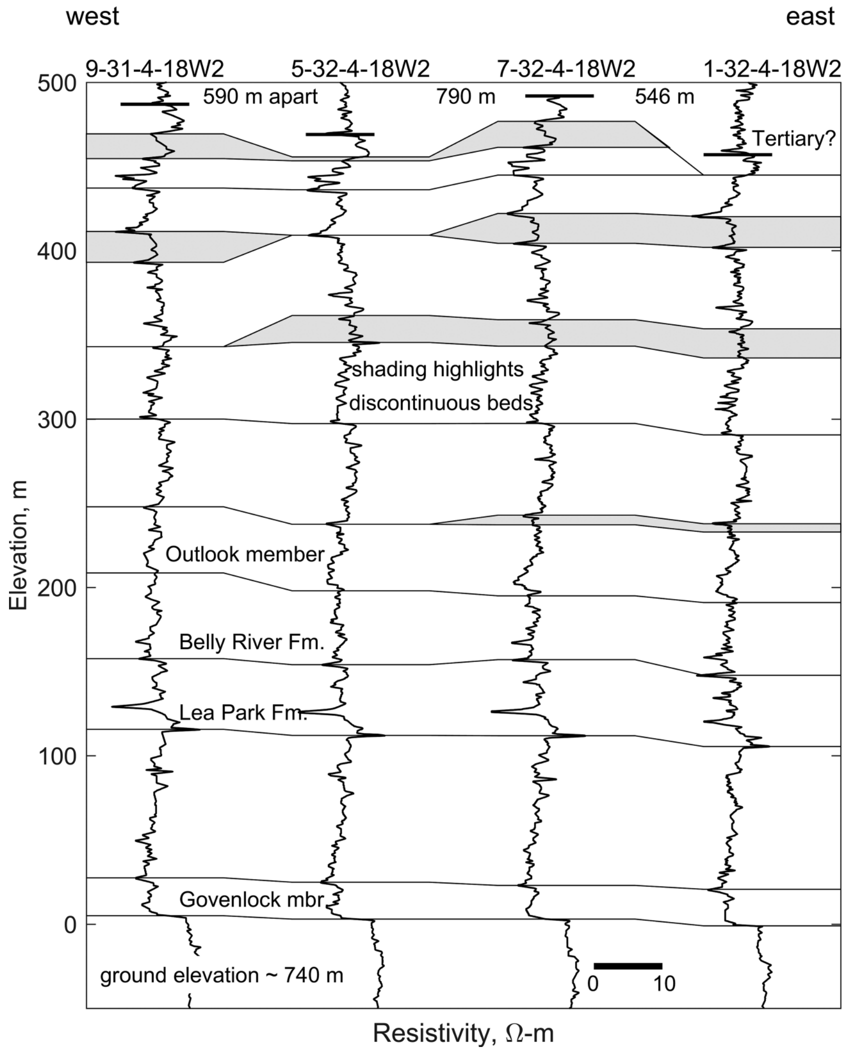

faulting should be recognized as a potential hazard when undertaking geotechnical analysis on the Great Plains where underlying Upper Cretaceous rocks exist. Engineering implications of the faults should be considered in the analysis of existing or potential road cuts, dam impoundments, building foundations, and natural slumping geotechnical considerations.

References

Bertog, J. 2010. Stratigraphy of the lower Pierre Shale (Campanian): implications for the tectonic and eustatic controls on facies distributions. Journal of Geological Research, **2010**: Article ID 910243. doi:10.1155/2010/910243.

Brooker, E.W., and Peck, R.B. 1993. Rational design treatment of slides in overconsolidated clays and clay shales. Canadian Geotechnical Journal, **30**(3): 526–544. doi:10.1139/t93-045.

Byers, A. 1959. Deformation of the Whitemud and Eastend Formations near Claybank. Saskatchewan, Transactions of the Royal Society of Canada, **53**, Series 3, Sect. 4, pp. 1–11.

Cartwright, J. 1994. Episodic basin-wide fluid expulsion from geopressured shale sequences in the North Sea Basin. Geology, **22**(5): 447–450. doi:10.1130/0091-7613(1994)022<0447:EBWFEF>2.3.CO;2.

Cartwright, J. 2011. Diagenetically induced shear failure of fine-grained sediments and the development of polygonal fault systems. Marine and Petroleum Geology, **28**(9): 1593–1610. doi:10.1016/j.marpetgeo.2011.06.004.

Cartwright, J. 2014. Are outcrop studies the key to understanding the origins of polygonal fault systems? Geology, **42**(6): 559–560. doi:10.1130/focus062014.1.

Cartwright, J., and Dewhurst, D. 1998. Layer-bound compaction faults in fine-grained sediments. Geological Society of America Bulletin, **10**(10): 1242–1257. doi:10.1130/0016-7606(1998)110<1242:LBCFIF>2.3.CO;2.

Cartwright, J.A., and Lonergan, L. 1996. Volumetric contraction during the compaction of mudrocks: a mechanism for the development of regional-scale polygonal fault systems. Basin Research, **8**(2): 183–193. doi:10.1046/j.1365-2117.1996.01536.x.

Cartwright, J.A., James, D.M.D., and Bolton, A. 2003. The genesis of polygonal fault systems: a review. *In* Subsurface sediment mobilization. *Edited by* P. Van Rensbergen, R.R. Hillis, A.J. Maltman, and C.K. Morley. Geological Society, London, Special Publications, **216**: 223–243. doi:10.1144/GSL.SP. 2003.216.01.15.

CBC News. 2011. Lawsuits filed over Deer Valley home. [Online.] Available from http://www.cbc.ca/news/canada/saskatchewan/lawsuits-filed-over-deer-valley-homes-1.1057046 [accessed on 6 August 2016].

CBC News. 2016. Regina Beach, Saskatchewan residents asking for help with slumping land. [Online.] Available from http://www.cbc.ca/news/canada/saskatchewan/regina-beach-residents-frustrated-with-slumping-land-1.3543986 [accessed on 6 August 2016].

Christiansen, E.A. 1967. Collapse structures near Saskatoon, Saskatchewan, Canada. Canadian Journal of Earth Sciences, **4**(5): 757–767. doi:10.1139/e67-053.

Christopher, J.E., and Yurkowski, M. 2004. Geological mapping of Mesozoic strata in southeastern Saskatchewan, northwestern North Dakota, and northeastern Montana, and regional effects of deformation by glacial-ice loading. *In* Summary of Investigations 2004. Vol. 1, Saskatchewan Geological Survey, Sask. Industry Resources, Misc. Rep. 2004-4.1, and CD-ROM. Available from http://publications.gov.sk.ca/documents/310/88844-chris.pdf [accessed 9 July 2016].

Cobban, W.A., Walaszczyk, Ireneusz, Obradovich, J.D., and McKinney, K.C. 2006. A USGS zonal table for the Upper Cretaceous middle Cenomanian-Maastrichtian of the Western Interior of the United States based on ammonites, inoceramids, and radiometric ages. U.S. Geological Survey Open-File Report 2006-1250, 45 p. Available from https://pubs.usgs.gov/of/2006/1250/pdf/OF06-1250_508.pdf [accessed 13 July 2016].

Collins, D., Swolfs, H., and Nichols, T. 1988. Highway damage related to faults near Pierre, South Dakota. USGS Open-File Report 88-674, 45 p. Available from https://pubs.er.usgs.gov/publication/ofr88674 [accessed 1 August 2016].

Cruden, D., and Tsui, P. 1991. Some influences of ice thrusting in geotechnical engineering. *In* Proceedings of the 25th Annual Conference of the Engineering Group of the Geological Society; Quaternary Engineering Geology. *Edited by* A. Forster, M.G. Culshaw, C. Cripps, J.A. Little, and C.F. Moon. Geological Society Engineering Geology Special Publication (1991), **7**: 127–134. doi:10.1144/GSL.ENG.1991.007.01.09.

Cruden, D.M., Thomsen, S., Kim, H.J., and Peterson, A.E. 1995. The Edgerton landslides. Canadian Geotechnical Journal, **32**(6): 989–1001. doi:10.1139/t95-097.

Davis, T.L. 1985. Seismic evidence of tectonic influence of development of Cretaceous listric normal faults, Boulder-Wattenberg-Greeley area, Denver Basin, Colorado. The Mountain Geologist, **22**(2): 47–54.

Erskine, C. 1973. Landslides in the vicinity of the Fort Randall Reservoir, South Dakota. USGS Geological Survey Professional Paper 675, 71 p. Available from https://pubs.usgs.gov/pp/0675/report.pdf [accessed 15 December 2016].

Gendzwill, D., and Stauffer, M. 2006. Shallow faults, Upper Cretaceous clinoforms, and the Colonsay Collapse, Saskatchewan. Canadian Journal of Earth Sciences, **43**(12): 1859–1875. doi:10.1139/e06-071.

Goodman, R. 1976. Methods of geological engineering in discontinuous rocks. West Publishing Company. ISBN: 0-8299-0066-7.

Goulty, N. 2008. Geomechanics of polygonal fault systems: a review. Petroleum Geoscience, **14**(4): 389–397. doi:10.1144/1354-079308-781.

Goulty, N., and Swarbrick, R. 2005. Development of polygonal fault systems: a test of hypotheses. Journal of the Geological Society, **162**(4): 587–590. doi:10.1144/0016-764905-004.

Hallberg, G., and Kemmis, T. 1986. Stratigraphy and correlation of the glacial deposits of the Des Moines and James lobes and adjacent areas in North Dakota, South Dakota, Minnesota, and Iowa. Quaternary Science Reviews, **5**: 65–68. doi:10.1016/S0277-3791(86)80010-5.

Hanczaryk, P., and Gallagher, W. 2007. Stratigraphy and paleoecology of the middle Pierre Shale along the Missouri River, central South Dakota. GSA Special Papers 2007, **427**: 51–69. doi:10.1130/2007.2427(04).

Hardenbicker, U. 2014. Esterhazy field trip guide. *In* Prairie perspectives: geographical essays. *Edited by* B. Thraves. Canadian Association of Geographers. Available from http://pcag.uwinnipeg.ca/Prairie-Perspectives/PP-Vol17/Hardenbicker.pdf [accessed 5 August 2016].

Hargrave, J. 2007. Pteranodon (Reptilia: Pterosauria): stratigraphic distribution and taphonomy in the lower Pierre Shale Group (Campanian), western South Dakota and eastern Wyoming. GSA Special Papers **427**: 215–225. doi:10.1130/2007.2427(16).

Henriet, J.P., Batist, M., and Verschuren, M. 1991. Early fracturing of Paleogene clays, southernmost North Sea: relevance to mechanisms of primary hydrocarbon migration. *In* Generation, accumulation and production of Europe's hydrocarbon. *Edited by* A.M. Spencer. Special Publications of the European Association of Petroleum Geologists, Vol. 1, pp. 217–227. Oxford University Press, Oxford.

Ito, M., and Azam, S. 2009. Engineering characteristics of a glacio-lacustrine clay deposit in a semi-arid climate. Bulletin of Engineering Geology and the Environment, **68**: 551–557. doi:10.1007/s10064-009-0229-7.

Kernan, N. 2015. Structural and facies characterization of the Niobrara Formation in Goshen and Laramie counties, Wyoming. Master's thesis, Colorado School of Mines, 131 p. Available from https://dspace.library.colostate.edu/bitstream/handle/11124/17082/Kernan_mines_0052N_10624.pdf?sequence=1&isAllowed=y [accessed 15 August 2016].

Kupsch, W. 1962. Ice-thrust ridges in western Canada. Journal of Geology, **70**: 582–590. doi:10.1086/626853.

Leonard, A. 1911. The Cretaceous and Tertiary formations of Western North Dakota and eastern Montana. The Journal of Geology, **19**(6): 507–547. Available from http://www.jstor.org/stable/30063538 [accessed 15 December 2016]. doi:10.1086/621886.

Lopez, T., Antoine, R., Darrozes, J., Rabinowicz, M., and Baratoux, D. 2015. Formation of polygonal fracture system as a result of hydrodynamic instabilities in clay-rich deposits. Geological Society of America Annual Meeting, Baltimore, Maryland. Available from https://gsa.confex.com/gsa/2015AM/webprogram/Handout/Paper267450/Poster_Clays_GSA15.pdf [accessed on April 16, 2016].

Maher, H. 2014. Distributed normal faults in the Niobrara Chalk and Pierre Shale of the central Great Plains of the United States. Lithosphere, **6**(5): 319–334. doi:10.1130/L367.1.

Meek, F.B., and Hayden, F.V. 1862. Descriptions of new lower Silurian (Primordial), Jurassic, Cretaceous, and Tertiary fossils collected in Nebraska Territory, with some remarks on the rocks from which they were obtained. Proceedings of the Academy of Natural Sciences of Philadelphia, **13**: 415–447.

Mittal, H., and Rahman, M. 2000. Stability of Alameda Dam during construction. *In* Proceedings - Canadian Dam Association Annual Conference, Regina.

Myers, V., Best, R., Dalsted, K., Devries, M., Eidenshink, J., Fowler, R., Heilman, J., and Schmer, F. 1980. Remote sensing applications to resource problems in South Dakota. Brookings Remote Sensing Institute, National Aeronautics and Space Administration, Washington, D.C. Available from https://ntrs.nasa.gov/archive/nasa/casi.ntrs.nasa.gov/19800011313.pdf [accessed on 23 December 2016].

Nichols, T.C., Jr., Collins, D.S., and Davidson, R.R. 1986. *In situ* and laboratory geotechnical tests of the Pierre Shale near Hayes, South Dakota—A characterization of engineering behavior. Canadian Geotechnical Journal, **23**(2): 181–914. doi:10.1139/t86-028.

Nichols, T.C., Jr. 1992. Rebound in the Pierre Shale of South Dakota and Colorado Field and laboratory evidence of physical conditions related to processes of shale rebound. USGS Open File Report 92-440. Available from https://pubs.usgs.gov/of/1992/0440/report.pdf [accessed on 5 August 2016].

Peterson, R. 1958. Rebound in the Bearpaw shale, western Canada. Geological Society of America Bulletin, **69**: 1113–124. doi:10.1130/0016-7606(1958)69[1113:RITBSW]2.0.CO;2.

Quinn, J., Chin, B., Pernito, M., and Scammell, J. 2014. Geotechnical assessment of Alameda Dam. *In* GeoRegina 2014: 67th Canadian Geotechnical Conference, Regina, Saskatchewan, September 28–October 2, 2014, Canadian Geotechnical Society.

Richmond, G., and Fullerton, D. 1986. Introduction to quaternary glaciations in the United States of America. Quaternary Science Reviews, **5**: 3–10. doi:10.1016/S0277-3791(86)80003-8.

Roberts, D., Crook, A., Cartwright, J., and Profit, M. 2015. Investigating the evolution of polygonal fault systems using geomechanical forward modeling. *In* The 49th US Rock Mechanics/Geomechanics Symposium held in San Francisco, Calif., USA, 28 June–1 July 2015.

Roberts, L., and Kirschbaum, M. 1995. Paleogeography of the Upper Cretaceous of the Western Interior of Middle North America- Coal distribution and sediment accumulation. USGS Professional Paper 1561, US Government Printing Office. Available from http://pubs.usgs.gov/pp/1561/report.pdf [accessed 16 April 2016].

Saskatchewan Geological Survey. 2016. Resource map of Saskatchewan, 2016 edition. Sask. Ministry of the Economy, Saskatchewan Geological Survey, Misc. Rep. 2016-1. Available from http://www.economy.gov.sk.ca/resourcemap [accessed August 5, 2016].

Sauer, E.K. 1978. The engineering significance of glacier ice-thrusting. Canadian Geotechnical Journal, **15**(4): 457–472. doi:10.1139/t78-051.

Sauer, E.K., Gareau, L.F., and Christiansen, E.A. 1990. Softening of overconsolidated Cretaceous clays by glacial erosion. Quarterly Journal of Engineering Geology and Hydrogeology, **23**: 307–324. doi:10.1144/GSL.QJEG.1990.023.04.05.

Schröder-Adams, C.J., Cumbaa, S.L., Bloch, J., Leckie, D.A., Craig, J., Seif El-Dein, S.A., Simons, D.-J.H., and Kenig, F. 2001. Upper Cretaceous (Cenomanian to Campanian) paleoenvironmental history of the Eastern Canadian margin of the Western Interior Seaway: bonebeds and anoxic events. Palaeogeography, Palaeoclimatology, Palaeoecology, **170**: 261–289. doi:10.1016/S0031-0182(01)00259-0.

Schultz, L., Tourtelot, H., Gill, J., and Boerngen, J. 1980. Composition and properties of the Pierre Shale and equivalent rocks, northern Great Plains region. USGS Professional Paper 1064, 123 p. Available from http://pubs.usgs.gov/pp/1064b/report.pdf [accessed 15 April 2016].

Shaw, R.J., and Hendry, M.J. 1998. Hydrogeology of a thick clay till and Cretaceous clay sequence, Saskatchewan, Canada. Canadian Geotechnical Journal, **35**(6): 1041–1052. doi:10.1139/t98-060.

Sonnenberg, S.A., and Underwood, D. 2013. Polygonal fault systems – a new structural style for the Niobrara Formation and Pierre Shale, Denver Basin, Colorado. Mountain Geologist, **50**(4): 127–142.

Stantec Consulting Ltd. 2016. 16TAN North Saskatchewan river Crossing – Geotechnical investigation Report (Final), 328 p. Available at http://publications.gov.sk.ca/documents/310/95830-16TAN%20North%20Sask%20River%20Crossing%20-%20Geotechnical%20Investigation%20Report%20-%20Stantec%20-%20November%203,%202016.pdf [accessed 14 December 2016].

Stauffer, M.R., and Gendzwill, D.J. 1987. Fractures in the northern plains, stream patterns, and the midcontinent stress field. Canadian Journal of Earth Sciences, **24**(6): 1086–1097. doi:10.1139/e87-106.

St-Onge, A. 2017. A Late Cretaceous polygonal fault system in central North America. Geological Society of America Bulletin. doi:10.1130/B31582.1.

Tewksbury, B., Hogan, J., Kattenhorn, S., Mehrtens, C., and Tarabees, E. 2014. Polygonal faults in chalk: insights from extensive exposures of the Khoman Formation, Western Desert, Egypt. Geology, **42**(6): 479–482. doi:10.1130/G35362.1.

Townsend, R. 1950. Deformation of Fort Union Formation near Lignite, North Dakota. Bulletin of the American Society of Petroleum Geologists, **34**: 1552–1564. [Online.] ISSN 1558-9153.

Twenhofel, W.H. 1925. Significance of some of the surface structures of central and western Kansas [with discussion]. AAPG Bulletin, **9**(7): 1061–1070.

Underwood, L.B., Thorfinnson, S.T., and Black, W.T. 1964. Rebound in design of Oahe Dam hydraulic structures. American Society of Civil Engineers, Journal of the Soil Mechanics and Foundations Division, **90**(2): 65–86.

Weimer, R. 1960. Upper Cretaceous Stratigraphy, Rocky Mountain area. American Association of Petroleum Geologists Bulletin, **44**(1): 1–20. [Online.] ISSN 1558-9153.

Witzke, B.J., and Ludvigson, G.A. 1994. The Dakota Formation in Iowa and the type area. *In* Perspectives on the Eastern Margin of the Cretaceous Western interior Basin. *Edited by* G. Shurr, G. Ludvigson, and R. Hammond. Geological Society of America Special Papers, 1994, 287, pp. 43–78. doi:10.1130/SPE287-p43.

Appendix A: Shallow seismic data geometry consideration

Exploration geophysicists use seismic data to image subsurface geological structures. Seismic data are acquired by initiating an

Pagination not final (cite DOI) / Pagination provisoire (citer le DOI)

Fig. A1. Vertical cross section showing source to receiver offset distance (*x*) geometry for seismic reflection from one layer.

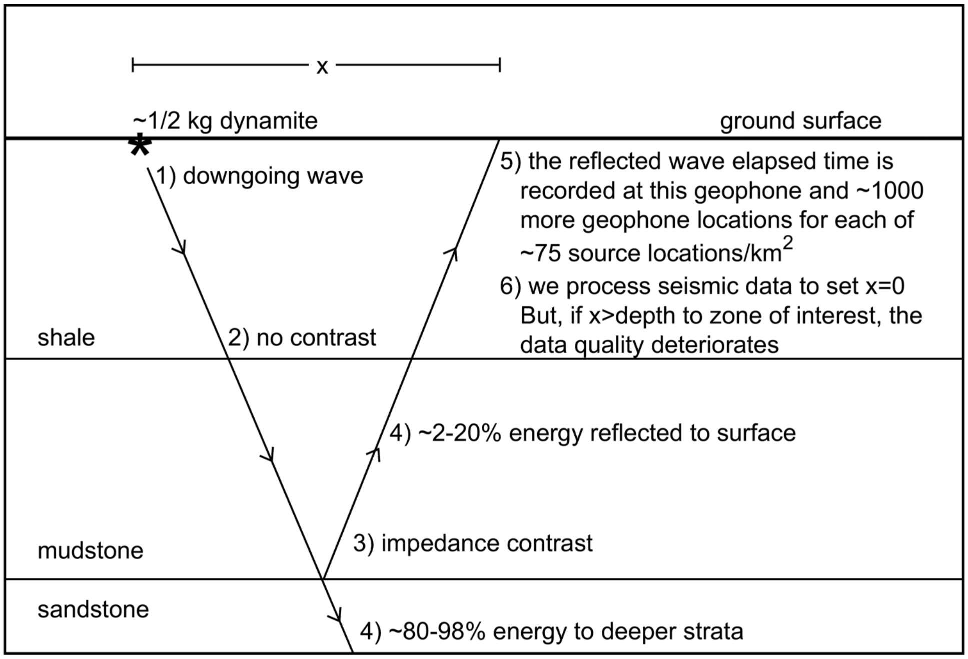

acoustic wave near ground surface, monitoring for reflected wave energy from below, and mapping the two-way traveltimes for those reflections. Acoustic waves are initiated at the ground surface using an energy source such as dynamite. In Saskatchewan, up to ~1000 geophones (each about the size of a pop can) are spiked into the ground at surveyed locations away from the dynamite source to record reflection arrival times by monitoring ground motion. Seismic data are processed to make a number of corrections for time delays caused by source and receiver acquisition geometry and other well-understood processes. The result is a data volume that can be interpreted to map relative structure for subsurface strata.

Part of the energy from a downgoing wave initiated at ground level will reflect back to ground surface if it encounters a change in acoustic impedance (Fig. A1). This can occur when strata with different bulk density or wave velocity overly each other. For example, shale with a low-velocity acoustic wave overlying a limestone with a high-velocity acoustic wave in the subsurface will reflect some of the energy from an incident acoustic wave back to the surface. The amount of reflected energy depends partly upon the acoustic wave velocity contrast between the two beds; a small change will result in a small reflection. If there is no impedance contrast at the bed contact, there will be no reflection of the wave energy, and the bed contact will not be imaged by the seismic data.

Geophone ground positions and source locations are spaced as far apart as possible to reduce data acquisition costs. In southeast Saskatchewan, the main targets of interest are at depths of 800–1600 m. This compares to the shallower zone of interest for the work presented here that has respective maximum depths of ~400–800 m. Cost-effective acquisition geometry for the deeper zones of interest makes the source to receiver offset *x* (Fig. A1) large for the shallower beds of interest here. Interpreting these shallower zones can be difficult, as the shallow data have poor signal to noise ratio and reduced lateral bed resolution when *x* is similar to the depth of the reflecting acoustic impedance contrast.

Appendix B: Gradient mapping

The fault traces (in Figs. 6 and 9) are taken from a gradient map computed using the respective two-way traveltime surfaces. The gradient map is the product of two 3 × 3 convolution masks, as defined by the Sobel edge enhancement masks (see Gao et al. 2010):

$$X = [-1\,0\,1,\ -2\,0\,2,\ -1\,0\,1]$$

$$Y = [-1\ -2\ -1,\ 0\,0\,0,\ 1\,2\,1]$$

A gradient map is computed by convolving a two-way traveltime map with the two 3 × 3 convolution masks, multiplying these numbers together, and plotting the gradient value at each map grid point. The gradient filter is effective in detecting large changes in the slope of a two-way traveltime map, such as where a fault occurs. The computed gradient values increase across faults with larger vertical offset. In this work, the gradient maps measure the rate of change for two-way traveltimes across gridded distances (where each cell in the map is 25 m in *x* or *y* direction). The gradient units for the fault traces in Figs. 6 and 9 are milliseconds per grid cell size or ms/25 m grid cell size.

Reference

Gao, W., Yang, L., Zhang, X., and Liu, H. 2010. An improved Sobel edge detection. *In* The 2010 3rd IEEE International Conference on Computer Science and Information Technology, pp. 67–71. doi:10.1109/ICCSIT.2010.5563693.